



Imaging Evaluation Following ^{90}Y Radioembolization of Liver Tumors: What Radiologists Should Know

Ijin Joo, MD¹, Hyo-Cheol Kim, MD¹, Gyoung Min Kim, MD², Jin Chul Paeng, MD³

Departments of ¹Radiology and ³Nuclear Medicine, Seoul National University Hospital, Seoul National University College of Medicine, Seoul 03080, Korea; ²Department of Radiology, Severance Hospital, Seoul 03722, Korea

Radioembolization using beta-emitting yttrium-90 microspheres is being increasingly used for the treatment of primary and metastatic liver cancers. It is a form of intra-arterial brachytherapy which delivers intense radiation to liver tumors with little embolic effect; this mode of action results in unique post-treatment imaging findings. It is important to understand these imaging findings to avoid misinterpretation of tumor response and to determine further management of the disease. Herein, we discuss the current concepts for assessing tumor response, common post-treatment imaging features, and associated complications following radioembolization.

Keywords: Radioembolization; Yttrium-90; Selective internal radiation therapy; Liver cancer; Post-treatment imaging

INTRODUCTION

Radioembolization, an increasingly used treatment option for primary and metastatic liver cancers, involves intra-arterial delivery of microspheres containing yttrium-90 (^{90}Y), a high-energy pure beta-emitter (1, 2). Technical similarity to chemoembolization may be deduced based on the term of "radioembolization"; however, this term is a misnomer given that radioembolization has little embolic effect (1). More specifically, chemoembolization exerts ischemic effects due to embolization and cytotoxic effects due to the use of chemotherapeutic drugs, whereas radioembolization works mainly via local radiation and needs blood flow to achieve

optimal radiation effects (3, 4).

As a form of brachytherapy, radioembolization can cause radiation-related changes in the adjacent structures around the target lesion (5, 6). Moreover, the delivery of radioactive microspheres to non-target organs can cause complications such as cholecystitis and gastrointestinal ulceration (5, 6). Familiarity with the imaging features of various post-treatment benign changes and potential pitfalls is important to avoid misinterpretation of these findings as tumor progression or other diseases.

In this review, we discuss the interpretation of imaging features following ^{90}Y radioembolization for liver malignancies including tumor response assessment, post-treatment benign changes, and potential complications. In addition, general strategies for pre-treatment evaluation and treatment procedures are presented to promote understanding of radioembolization.

Pre-Treatment Evaluation of Radioembolization

General Principles

During the selection of patients for radioembolization, a multidisciplinary approach involving experts who have

Received July 23, 2017; accepted after revision November 3, 2017.

Corresponding author: Hyo-Cheol Kim, MD, Department of Radiology, Seoul National University Hospital, 101 Daehak-ro, Jongno-gu, Seoul 03080, Korea.

• Tel: (822) 2072-2584 • Fax: (822) 743-6385
• E-mail: angiointervention@gmail.com

This is an Open Access article distributed under the terms of the Creative Commons Attribution Non-Commercial License (<http://creativecommons.org/licenses/by-nc/4.0>) which permits unrestricted non-commercial use, distribution, and reproduction in any medium, provided the original work is properly cited.

expertise in radiology, nuclear medicine, hepatology, radiation, medical, and surgical oncology is needed to select the optimal candidates (7). Patients should complete comprehensive evaluation of tumor burden, hepatic reserve, and performance status. Unresectable liver-only or liver-dominant primary or metastatic liver malignancies are considered good candidates for radioembolization (7), and intrahepatic tumor burden $\leq 70\%$ of the liver volume is generally considered to be acceptable (8). With respect to liver function, total bilirubin < 2.0 mg/dL and Child-Pugh class A-B7 would be required to tolerate the treatment (9, 10). In addition, life expectancy ≥ 12 weeks and European Cooperative Oncology Group status 0–2 would be acceptable for radioembolization (7). In Korea, since ^{90}Y microspheres are not reimbursed by the national health insurance, patients' economic status and their private health insurance are also important factors that determine the treatment options.

Screening Test: Hepatic Angiography and $^{99\text{m}}\text{Tc}$ -MAA Scan

Patients who are selected as candidates for radioembolization of liver tumors should undergo pretreatment simulation tests consisting of hepatic angiography and technetium-99m macroaggregated albumin ($^{99\text{m}}\text{Tc}$ -MAA) scan (6).

On preparatory angiography, the anatomy of the hepatic artery and the presence of non-hepatic arteries originating from the hepatic artery are investigated. Recently, C-arm cone-beam computed tomography has become an essential tool for angiographic evaluation that is particularly useful to visualize small arteries (11). Angiographic information

is critical because if radioactive microspheres are infused into the non-hepatic arteries during radioembolization procedures, serious complications such as gastrointestinal ulcers can occur (6). Thus, prophylactic embolization of non-target branch vessels, including an accessory left gastric artery, right gastric artery, hepatic falciform artery, and esophageal branches from the replaced left hepatic artery, can be performed, although there are controversies about the indications (9, 12, 13).

Technetium-99m macroaggregated albumin scans aim to estimate extrahepatic deposition and lung shunting by simulating the microsphere biodistribution of ^{90}Y (14). Immediately after $^{99\text{m}}\text{Tc}$ -MAA is injected into the hepatic artery in the angiography suite, patients are transferred to gamma camera for a lung shunt scan with or without single photon emission computed tomography (SPECT)/CT. Although SPECT/CT is not essential in dosimetry, it can provide more reliable assessment of $^{99\text{m}}\text{Tc}$ -MAA distribution on fusion images (Fig. 1), which may be useful to predict tumor response, to detect unexpected perfusion outside of the liver, and to elaborate dosimetry of the partition model (15). If radioactivity is detected in the non-target organs on $^{99\text{m}}\text{Tc}$ -MAA scan, prophylactic embolization can be performed or catheter position can be modified at the time of the procedure to avoid severe complications (13). Lung shunting is one of the major concerns of radioembolization because radiation pneumonitis can develop in case of an excessive intratumoral arteriovenous shunt (16). For the two commercially available ^{90}Y products including TheraSphere[®] glass microspheres (BTG, London, UK) and

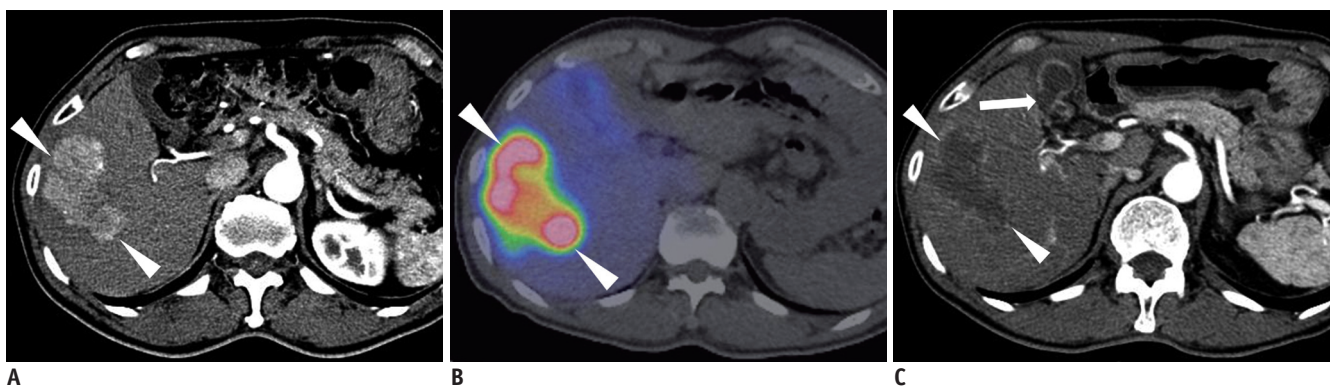


Fig. 1. 67-year-old man with HCC.

A. Pre-treatment CT image shows hypervascular tumor in right lobe of liver. **B.** $^{99\text{m}}\text{Tc}$ -MAA SPECT/CT after delivery of $^{99\text{m}}\text{Tc}$ -MAA into right hepatic artery shows high activity in tumor (arrowheads) but weak activity in liver parenchyma, which would predict good response to radioembolization. **C.** CT scan of arterial phase 1 month after ^{90}Y radioembolization shows loss of enhancement in tumor, suggesting tumor necrosis (arrowheads). Note wall edema and mucosal rent of gallbladder (arrow). Despite this abnormal imaging finding of gallbladder, this patient did not have any clinical symptoms or laboratory abnormality suggesting acute cholecystitis, and therefore, no interventional treatment was performed for gallbladder. HCC = hepatocellular carcinoma, SPECT = single photon emission computed tomography, $^{99\text{m}}\text{Tc}$ -MAA = technetium-99m macroaggregated albumin

SIR-Spheres[®] resin microspheres (Sirtex Medical, North Sydney, Australia), lung dose of 30 Gy for a single treatment and 50 Gy as a cumulative dose for TheraSphere[®] (6), and 20% lung shunting for SIR-Spheres[®] are the recommended upper limits (17).

If a patient is determined to be eligible to receive radioembolization, intra-arterial delivery of radioactive microspheres is commonly performed 1 or 2 weeks after the screening tests (1).

Treatment Methods

The procedure techniques of radioembolization are quite similar to those of chemoembolization, since both techniques require selective catheterization of the hepatic artery and involve transarterial delivery of therapeutic particles. However, radioembolization is usually performed in a less selective fashion compared to chemoembolization. In patients with localized disease, radioactive microspheres are administered via a segmental or lobar hepatic artery according to the tumor extent and liver function (18). In patients with multiple hepatocellular carcinomas (HCCs) or metastases of bilobar involvement, radioactive microspheres are usually infused at the lobar artery level with sequential split treatment (i.e., treating one lobe in the 1st session and then the other lobe in the 2nd session with a 4–6 week interval) to reduce treatment-related complications (18).

Radiation segmentectomy refers to radioembolization involving 2 or fewer hepatic segments by injection of radioactive microspheres at a high ablative dose into segmental hepatic arteries, which may result in complete necrosis of the tumor as well as non-tumorous hepatic

parenchyma of a treated segment (19, 20). A segment treated by radiation segmentectomy gradually shrinks and it often looks like a surgical segmentectomy on follow-up imaging (21).

Radiation lobectomy represents injection of radioactive microspheres at a regular dose into a lobar artery to induce contralateral lobe hypertrophy (22, 23). This can be used as a bridge to liver resection in patients who initially have a small future liver remnant volume. Until now, portal vein embolization has been widely used as a standard technique for this purpose. Compared to portal vein embolization, radioembolization provides the potential benefit of offering concomitant control of liver tumors during the waiting time (23).

Immediate Post-Treatment ⁹⁰Y PET Imaging

Although ⁹⁰Y is a pure beta-emitter, it emits very small amount of positron (0.003%) and, therefore, can be imaged by sensitive positron emission tomography (PET) scanners (24). Immediately after radioembolization, ⁹⁰Y PET can demonstrate the actual distribution of radioactive microspheres (Fig. 2), and the absorbed radiation dose to each part of the lesion can be estimated (25). Therefore, ⁹⁰Y PET imaging including PET/CT and PET/MR imaging may be useful in the prediction of tumor response as well as in the interpretation of follow-up imaging (26, 27).

Tumor Response Assessment for Radioembolization

Size- and Tumor Viability-Based Imaging Criteria

Effective radioembolization would finally induce reduction

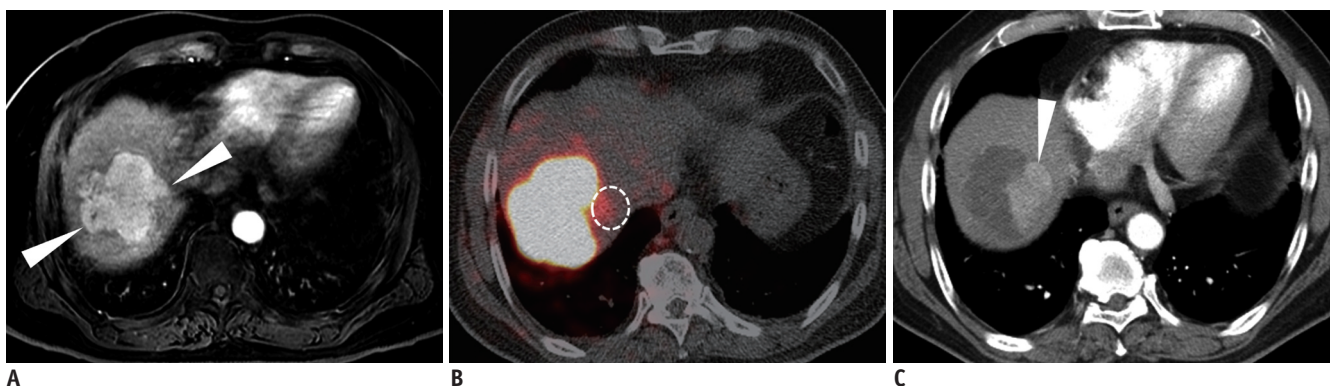


Fig. 2. 68-year-old man with HCC.

A. Pre-treatment MR image shows large hypervascular mass (arrowheads) in right lobe of liver. **B.** PET/CT image immediately after ⁹⁰Y radioembolization demonstrates high activity of ⁹⁰Y microspheres in tumor. Note defect in activity in medial part of tumor (dotted circle). **C.** CT scan taken 1 month after ⁹⁰Y therapy shows intra-tumoral nodular enhancement in medial portion (arrowhead). This lesion had grown up slowly on subsequent CT scan, and was treated by chemoembolization 6 months after ⁹⁰Y radioembolization. PET = positron emission tomography, ⁹⁰Y = yttrium-90

in the size of the tumor, and this size-based response can be useful in the prediction of survival outcomes (28, 29). However, the decrease in size after radioembolization occurs slowly, with a reported median time to response of 4–6 months according to the WHO criteria for responding patients with HCC (30, 31). On the other hand, tumor viability-based imaging criteria such as modified response evaluation criteria in solid tumor and European Association for the Study of Liver (EASL) criteria may enable earlier and more sensitive detection of tumor response to radioembolization than size-based criteria (31, 32), and can be useful in the prediction of pathologic complete response (33). Moreover, responders identified based on tumor viability-based imaging criteria have been reported to show favorable overall survival after radioembolization of liver tumors (30, 34, 35).

While an increase in tumor size is usually regarded as

a finding suggestive of tumor progression, a paradoxical increase in tumor size at an early follow-up after radioembolization should be interpreted with caution because it can be caused by intra-tumoral hemorrhage, edema, and necrosis (Fig. 3) (36, 37). In addition, tumor growth increment during the time interval from pre-treatment imaging to the administration of ^{90}Y can also cause size discrepancy between pre- and post-treatment imaging. Usually, it takes 3–4 weeks from the initial imaging study to radioembolization, because there are multiple required steps before treatment, including simulation test, hospital admission, and delivery of radioactive microspheres from the manufacturing facility.

On an early follow-up, persistent tumoral enhancement or residual enhancing areas are common imaging features (Fig. 4), and they do not have a predictive value for viable tumor (37). While a decrease in the degree of tumor enhancement

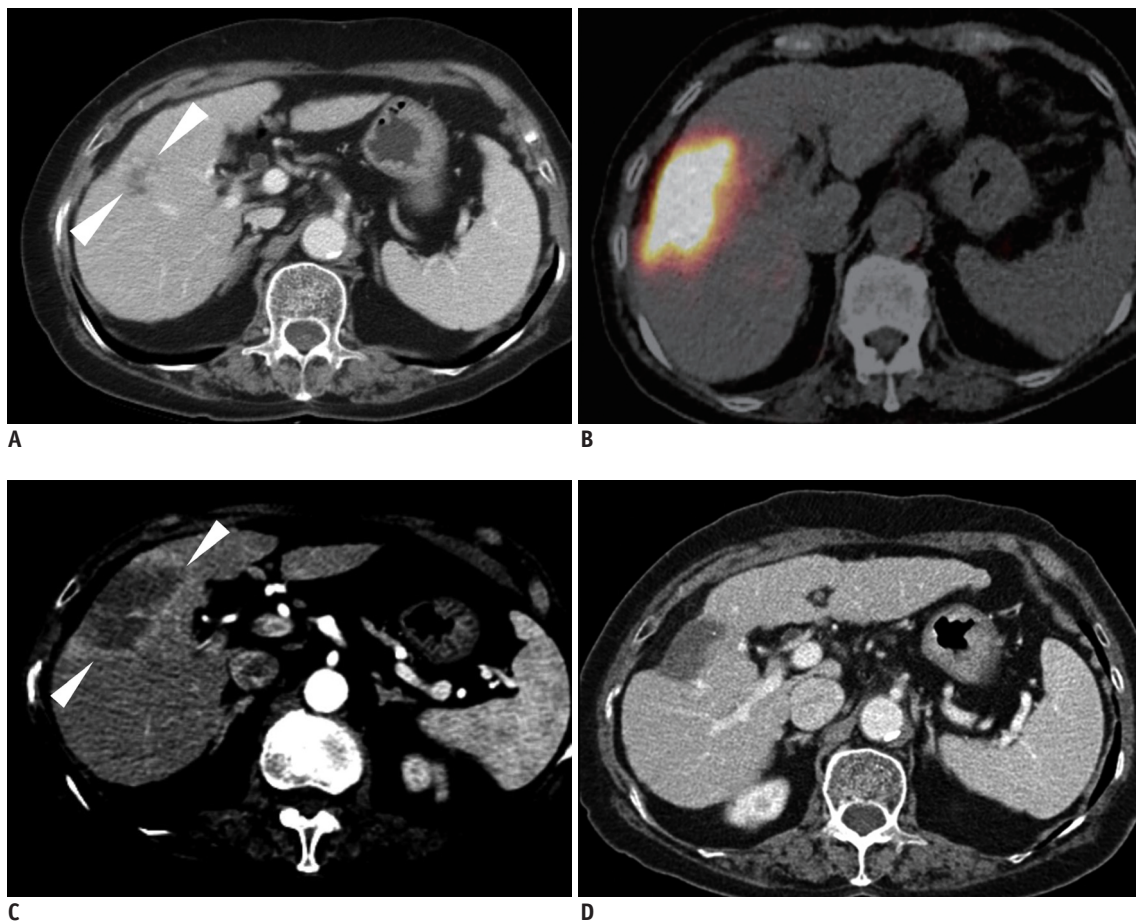


Fig. 3. 80-year-old woman with intrahepatic cholangiocarcinoma.

A. Pre-treatment CT scan shows 3.5 cm mass (arrowheads) in right lobe of liver. **B.** PET/CT image immediately after ^{90}Y radioembolization reveals high activity in tumor as well as in surrounding hepatic parenchyma. **C.** Arterial phase CT image 2 months after ^{90}Y radioembolization shows 7 cm low-attenuating area (arrowheads) in treated lobe that may represent necrosis of tumor and peritumoral parenchyma. This size discrepancy between pre- and post-treatment images should not be interpreted as tumor progression. **D.** One year follow-up CT image shows shrinkage of treated lesion with liver surface retraction.

is a finding suggestive of effective treatment, this change usually takes several months after radioembolization (38). Reactive edema and granulation tissue formation after treatment may result in enhancement without a viable tumor (36). A recent study showed that pathologic complete response was not infrequent in cases that show a partial response according to EASL criteria (33). Therefore, differentiation of a non-responding viable tumor from the well-responding portion is often challenging on contrast-enhanced imaging. Although the clinical indication for an additional intervention has not been well established (39), if the enhancing part increases on a serial follow-up, it is generally regarded as a viable tumor requiring additional therapy (Fig. 5). On the contrary, if the enhancing part does not show interval increase paralleled by a stable or decrease in serum tumor marker levels, it can be observed without

further treatment.

Diffusion-Weighted MR Imaging

Diffusion-weighted MR imaging (DWI), which reflects tissue cellularity and integrity of the cell membrane, can provide functional information about the tumor (40). As alterations in DWI-derived parameters can precede the morphologic changes in the tumor after treatment, they can be useful in the early prediction of tumor response speeding up the “go or no-go” decision making process (40).

In the monitoring of tumor response after radioembolization, tumor necrosis after effective treatment corresponds to an increase in the apparent diffusion coefficient (ADC) value of the tumor (Fig. 6) (41). For liver tumors treated with radioembolization, there have been several reports showing that greater increase in tumor ADC



Fig. 4. 82-year-old man with HCC.

A. Pre-treatment CT scan shows hypervascular mass (arrowheads) in left lobe of liver. **B.** CT scan 2 months after ^{90}Y therapy shows persistent enhancement of tumor (arrowheads). Tumor size was slightly decreased. **C.** CT scan 6 months after ^{90}Y radioembolization shows reduced tumor size and decreased tumor enhancement (arrowheads). CT scan 1 year after ^{90}Y radioembolization shows further decrease in size and enhancement of tumor (data not shown). This patient did not receive any additional treatment.

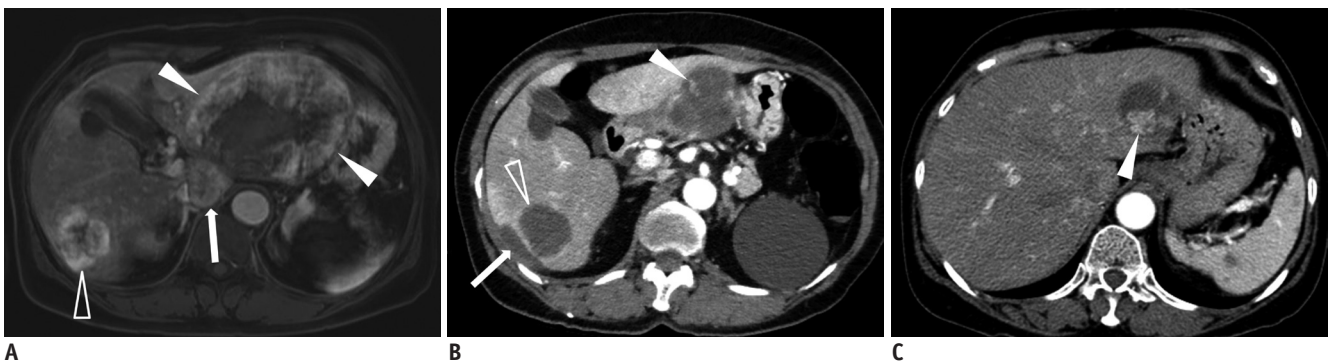


Fig. 5. 57-year-old woman with liver metastases from neuroendocrine tumor.

A. Pre-treatment MR image shows 10 cm tumor (arrowheads) in left lobe of liver, 3 cm tumor in caudate lobe (arrow), and 4 cm tumor in right lobe (open arrowhead). **B.** CT scan 1 month after ^{90}Y radioembolization shows loculated perihepatic ascites (arrow) beside right lobe. Note disappearance of enhancement of tumor in right lobe (open arrowhead) and residual enhancing portion of tumor in left lobe (arrowhead). As residual enhancement on early follow-up is common imaging feature, no additional treatment was performed for this finding. **C.** CT scan 11 months after ^{90}Y radioembolization demonstrates increased enhancing nodular lesion (arrowhead) within treated tumor which suggests tumor recurrence. Chemoembolization was performed using iodized oil, and follow-up image shows nodular dense accumulation of iodized oil within recurrent tumor (data not shown).

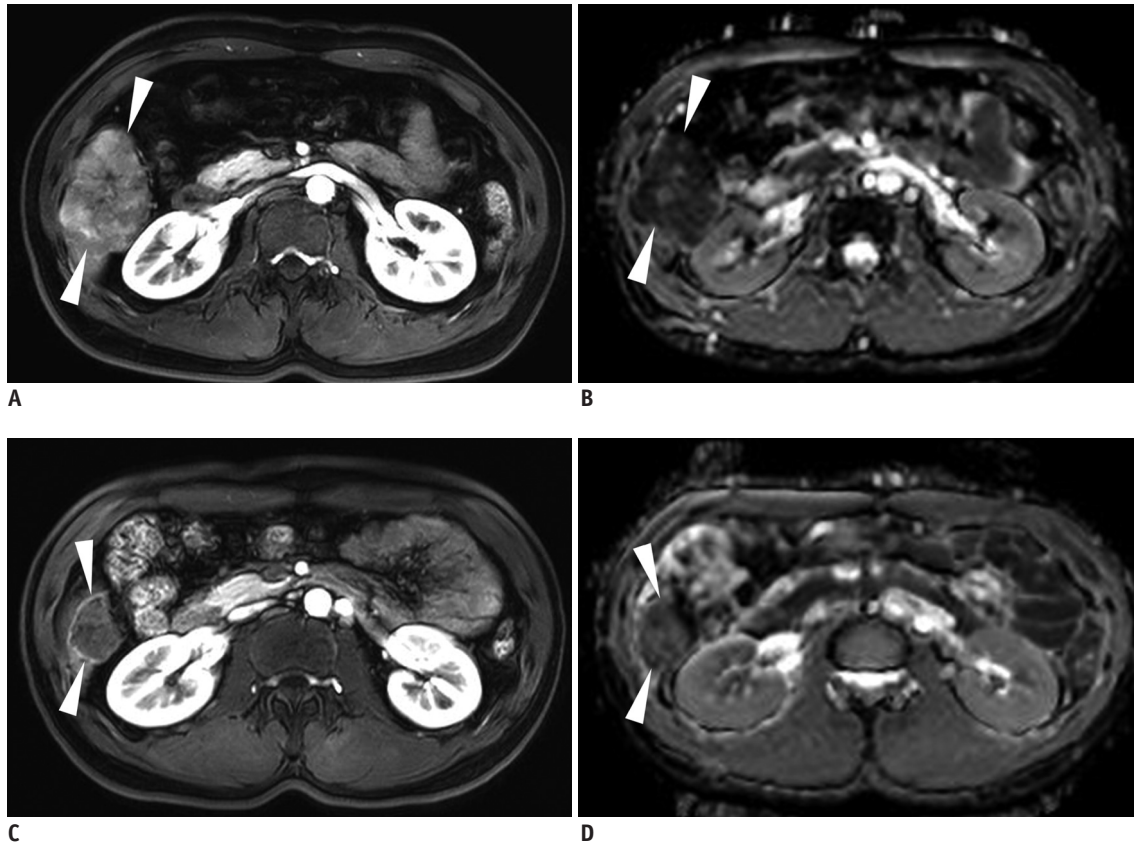


Fig. 6. 37-year-old man with HCC.

Pre-treatment MRI shows hypervascular mass (arrowheads) in segment VI of liver on arterial phase (A) which shows low ADC value of 0.95 mm²/sec (B). On post-radioembolization MRI, mass (arrowheads) shows decrease in size, decrease in arterial enhancement, and peritumoral ring enhancement (C), and increase in ADC value of 1.45 mm²/sec of tumor (arrowheads) (D) which are findings suggestive of good response to treatment. ADC = apparent diffusion coefficient

on early follow-up may be a favorable predictor for the later tumor response and survival outcome (42, 43). In addition, both cellular swelling immediately after treatment and increased cellularity due to tumor progression can cause reduction in the ADC value (41, 44), interpretation of tumor ADC should be performed with caution according to the follow-up interval after treatment.

Intravoxel incoherent motion (IVIM)-DWI, which is based on the concept of bi-exponential signal decay as a function of b values, is receiving increasing attention as a quantitative tool for assessing tumor response (44-46). As IVIM-DWI can estimate microcirculation and molecular diffusion separately, it might be useful in the evaluation of changes in tissue perfusion, cellularity, and necrosis after anti-cancer treatment (45). Recent studies have shown the potential usefulness of perfusion-related parameters derived from IVIM-DWI as early predictors of prognosis in patients with hepatic metastases after radioembolization (47, 48).

Tumor Marker

The levels of serum tumor markers (e.g., alpha-fetoprotein in HCC, carcinoembryonic antigen in colorectal liver metastases, and carbohydrate antigen 19-9 in intrahepatic cholangiocarcinoma) generally decrease after radioembolization (29, 49, 50). Response classification based on the tumor markers may correlate with future imaging response and survival outcomes (49, 51). However, the time-dependent change in a tumor marker does not always correspond to the imaging response (52). The response of tumor markers usually precedes the response of imaging, and combined interpretation of a tumor marker and imaging during follow-up after radioembolization may provide more accurate information about the need for additional treatment. As discussed earlier in this article, when interpreting persistent enhancement on an early follow-up, responders and non-responders for tumor markers may have different probabilities for the presence of a pathologically viable tumor.

Benign Post-Treatment Imaging Findings

Radiation Effect on Non-Tumorous Hepatic Parenchyma

While microspheres are preferentially deposited in hepatic tumors (53), non-tumorous hepatic parenchyma around the tumor and in the vascular territory of the treated segment is exposed to irradiation, and thus, may present radiation-induced changes. This finding usually appears without significant clinical manifestations or alteration in liver function tests (52).

Imaging features of radiation effect on hepatic parenchyma after radioembolization have not yet been well described. However, radiation-induced changes in the liver after external radiation have been reported in the previous studies (54-56) and can be applied in the interpretation of post-radioembolization examinations with caution. After external radiation therapy, the irradiated hepatic parenchyma frequently shows arterial hyper-enhancement on an early follow-up until 6 months which may interfere with accurate assessment of tumor response in HCC (54). Lack of washout appearance on the delayed phase can be helpful in differentiating radiation effect from tumor progression (54). On the portal venous phase and delayed phase images, the irradiated hepatic parenchyma can present various enhancement patterns according to the radiation dose and time interval after the treatment (55). Typical time-dependent changes are as follows: type I (within 3 months), hypo-attenuation on the portal venous phase and iso-attenuation on the delayed phase (Fig. 7B); type II (3-6 months), hypo-attenuation on the portal venous phase and hyper-attenuation on the delayed phase (Fig. 7C); type III (after 6 months), iso- or hyper-attenuation on the portal venous phase and hyper-attenuation on the

delayed phase (Fig. 8C) (55). Type I and II enhancement patterns may be explained by the radiation-induced acute veno-occlusive disease, resulting in delayed contrast inflow without and with reduced contrast clearance (56). Type III enhancement patterns may be related to distortion of the liver architecture and fibrotic change (55). By reflecting the time-dependent changes, serial imaging studies may show a shift in the enhancement patterns. In addition, the volume of hepatic parenchyma showing a radiation effect is usually decreased on an additional follow-up (56) (Figs. 7, 8).

Gadoxetic acid-enhanced MRI can provide functional information about hepatocyte uptake and, therefore, it may be useful in the detection and evaluation of the extent of radiation effect in the hepatic parenchyma. The irradiated hepatic parenchyma may show decreased signal intensity on hepatobiliary phase imaging of gadoxetic acid-enhanced MRI (Fig. 9). Value of hepatobiliary phase imaging following radioembolization should be further validated in terms of correlation with clinical manifestations and prognosis.

Radiation Necrosis of the Hepatic Parenchyma

During radiation segmentectomy, excessive high dose radiation is selectively delivered into the focal area of the liver, and it may lead to necrosis, not only in the tumor but also in the hepatic parenchyma of the treated segment (Fig. 3) (52). Radiologically, hepatic parenchyma showing radiation necrosis shows poor or no enhancement, and shrinks with passage of time. Focal radiation necrosis should not be misdiagnosed as a new hypovascular tumor or progression of the previous disease. By showing the distribution of radioactive microspheres, ⁹⁰Y PET following radioembolization can help in the differential diagnosis. If the matched area shows high activity on ⁹⁰Y PET, radiation



Fig. 7. 79-year-old man with intrahepatic cholangiocarcinoma.

A. Pre-treatment CT scan of portal venous phase (left) and delayed phase (right) shows small tumor in right lobe (arrowhead). Radioactive microspheres were injected into right hepatic artery (data not shown). **B.** CT scan of portal venous phase (left) and delayed phase (right) 2 months after ⁹⁰Y radioembolization shows low attenuation on portal venous phase and iso-attenuation on delayed phase of right lobe, indicating type I radiation change. Note mild shrinkage of right lobe and hypertrophy of left lobe. **C.** CT scan of portal venous phase (left) and delayed phase (right) 4.5 months after ⁹⁰Y radioembolization shows low attenuation on portal venous phase and high attenuation on delayed phase of right lobe, indicating type II radiation change. Note progression of shrinkage of right lobe and hypertrophy of left lobe.

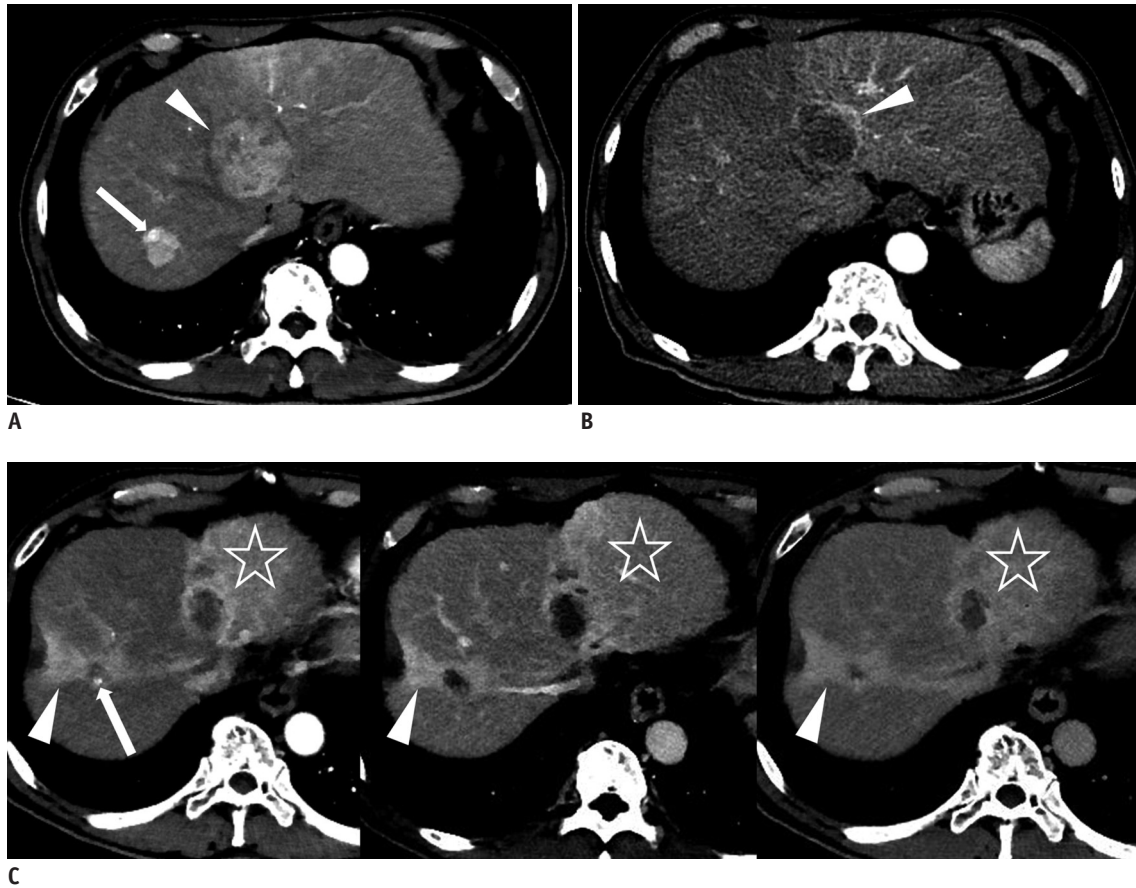


Fig. 8. 67-year-old man with HCC.

A. Pre-treatment CT scan shows large tumor in left lobe (arrowhead) and small tumor in right lobe (arrow). Radiation segmentectomy of segment VIII and radiation lobectomy of left lobe were performed in one session. **B.** CT scan of arterial phase 2 months after ^{90}Y radioembolization shows peritumoral ring enhancement (arrowhead) in left lobe. Due to suspicion of residual tumor, chemoembolization was requested. But, angiography failed to demonstrate tumor staining (data not shown), and therefore, no additional treatment was performed. **C.** CT scan of arterial phase (left), portal venous phase (middle), and delayed phase (right) 8 months after ^{90}Y radioembolization shows persistent peritumoral ring enhancement around left lobe tumor and dystrophic intratumoral calcification (arrow) in right lobe tumor. Note wedge-shaped enhancement (arrowhead) around right lobe tumor and diffuse enhancement (star) of left lateral segment with decreased volume of treated area, indicating type III radiation change after radiation segmentectomy and radiation lobectomy, respectively. At 16 month follow-up after ^{90}Y radioembolization, this patient has demonstrated no evidence of tumor recurrence on tumor marker and imaging studies (data not shown).

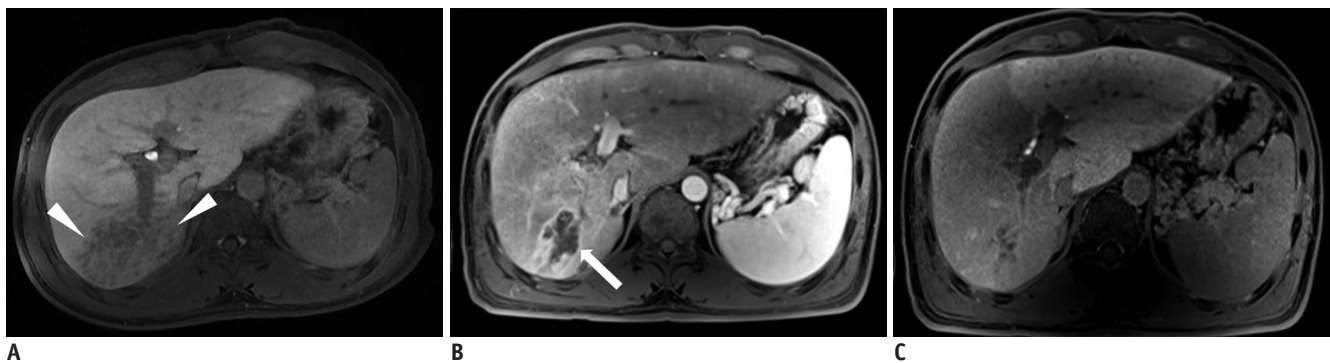


Fig. 9. 48-year-old man with HCC.

Pre-treatment gadolinium-enhanced MR image of hepatobiliary phase (20 minutes) (**A**) shows infiltrative tumor (arrowheads) in segment VII of liver. Radioactive microspheres were injected into right hepatic artery (data not shown). On gadolinium-enhanced MRI 3 months after ^{90}Y therapy, arterial phase image (**B**) demonstrates tumor necrosis (arrow) in segment VII and heterogeneous parenchymal enhancement of right lobe, and hepatobiliary phase image (20 minutes) (**C**) shows diffuse hypointensity of hepatic parenchyma in right lobe which may indicate radiation effect. This parenchymal change should not be misinterpreted as progression of infiltrative tumor.

necrosis should be considered as a differential diagnosis for the new hypovascular lesion (Fig. 10).

Peritumoral Ring Enhancement

After loco-regional treatment of hepatic tumors, nodular or peripheral ring-like enhancement around the treated lesion is usually considered to indicate local recurrence or a residual viable tumor (57). However, this may not be true following radioembolization. Peritumoral ring enhancement is frequently seen after radioembolization and it may persist for several months (Fig. 8) (31, 33). This finding is suggestive of a pathologic complete response with a high positive predictive value rather than the presence of a residual viable tumor (33). Pathologically, this imaging finding would correspond to granulation tissue related to the inflammatory treatment response and/or a fibrous pseudocapsule surrounding the tumor (58). Thus, this imaging finding should not be misinterpreted as local recurrence or a residual viable tumor. While peritumoral ring enhancement commonly shows circumferential enhancement with even thickness without wash-out on the portal venous and delayed phases, a marginal recurrent tumor shows nodular enhancement with wash-out.

Perivascular Edema

Transient perivascular edema is often seen 3–6 months after radioembolization, probably due to the deposition of microspheres in the peritumoral vascular plexus (51). It manifests as low-attenuating lesions with perivascular distribution on contrast-enhanced imaging studies (Fig. 11). Without knowledge of this transient phenomenon, it can be mistaken for an infiltrative tumor, which leads to an incorrect diagnosis of tumor progression, or for a hepatic attenuation change arising from a vascular problem (52). When low-attenuating lesions with perivascular distribution occur, and if the serum tumor marker level decreases without progression of the primary tumor, perivascular edema can be diagnosed easily.

Contralateral Lobe Hypertrophy

Radioembolization induces contralateral lobe hypertrophy of the untreated lobe and concomitant atrophy of the ipsilateral hepatic lobe (Fig. 7), which may be explained by the radiation effect and alteration in portal venous flow (5). The degree of hypertrophy of the contralateral lobe has been reported to be greater after radioembolization than after chemoembolization, and therefore, radioembolization

may have an advantage as a bridge to liver resection (22, 23, 59). Moreover, during the time to contralateral lobe hypertrophy, radioembolization has the potential to attain local tumor control (23).

Changes in the Gallbladder Wall

Gallbladder wall edema, mural hyper-enhancement, and mural rent (Fig. 1C) are common benign findings after radioembolization and they usually do not have any clinical consequences (6, 60). These changes may be due to the aberrant embedment of radioactive microspheres in the gallbladder wall through the cystic artery or small perforator arteries (52). The diagnosis of radiation cholecystitis should be made prudently even in cases of radiologic abnormality of the gallbladder, which will be described further in detail.

Perihepatic Fluid Collection and Pleural Effusion

Adjacent structures such as pleura and liver capsule may also be exposed to radiation, resulting in a small amount of perihepatic ascites (Fig. 5B) and pleural effusion, particularly in cases of tumors adjacent to the Glisson's capsule or the right pleura (51). They are regarded as transient reactive changes, and do not require any specific treatment. The appearance of perihepatic ascites and pleural effusion on follow-up imaging without any clinical symptoms or laboratory abnormality should not be misinterpreted as radioembolization-induced liver disease (REILD), indicating hepatic toxicity after radioembolization (5).

Dystrophic Calcification

Intratumoral dystrophic calcification can develop after radioembolization, probably secondary to tumor necrosis or degenerative changes (61). Dystrophic calcification can be easily identified as a high attenuated lesion within the tumor on CT images (Fig. 10D). This finding is occasionally encountered in colorectal liver metastases after chemotherapy and/or radiation therapy (61, 62). However, little is known about the predictive value of intratumoral dystrophic calcification after radioembolization with respect to pathologic tumor response or survival outcomes.

Complications

REILD

Radioembolization-induced liver disease may develop in 0–4% of cases after radioembolization due to exposure of the hepatic parenchyma to a high dose of radiation

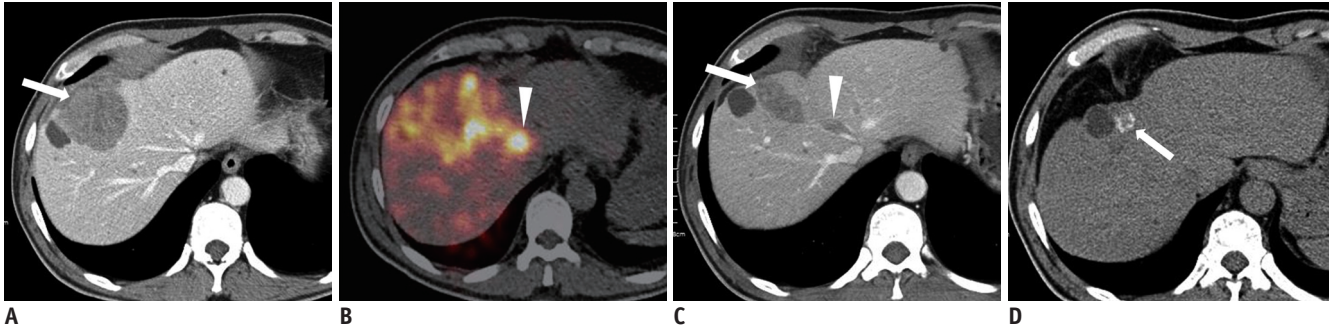


Fig. 10. 53-year-old man with HCC.

A. Pre-treatment CT image of portal venous phase demonstrates large tumor in segments IV and VIII of liver (arrow). **B.** On PET/CT immediately after ^{90}Y radioembolization, not only tumor but also hepatic parenchyma of segment IV between middle and left hepatic veins (arrowhead) shows increased activity suggesting high uptake of ^{90}Y microspheres. During procedure of ^{90}Y radioembolization, excessive ^{90}Y microspheres were delivered into small tumor-feeding artery whose vascular territory covered this area (data not shown). **C.** CT scan 3 months after ^{90}Y radioembolization shows shrinkage of hepatic tumor (arrow). Note new hypo-attenuating lesion (arrowhead) between middle and left hepatic veins with decrease in volume, which is thought to be radiation necrosis of hepatic parenchyma. This lesion should not be misdiagnosed as new hypovascular tumor. **D.** CT scan 8 months after ^{90}Y radioembolization shows shrinkage of hepatic tumor with dystrophic calcification (arrow).

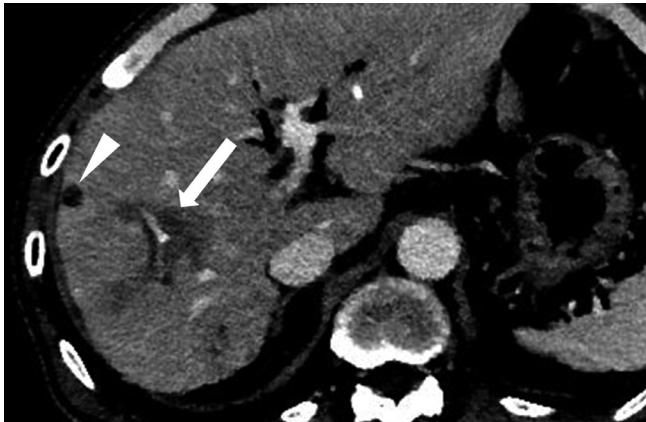


Fig. 11. 59-year-old man with hepatic metastases from pancreatic neuroendocrine tumor. CT scan 3 months after ^{90}Y radioembolization shows new low-attenuating lesions (arrow) with perivascular distribution in right lobe of liver. This finding is due to perivascular edema related to ^{90}Y radioembolization, which should not be misdiagnosed as infiltrative tumor. Note loss of enhancement of tumor (arrowhead).

(6). As the embolic effect of radioembolization is minimal, ischemic change due to embolization would not significantly contribute to liver damage (63). Contributing risk factors include underlying liver cirrhosis and previous or subsequent exposure to systemic chemotherapy (64). REILD may manifest with a wide spectrum of clinical manifestations, including abdominal pain, jaundice, and ascites, and laboratory abnormalities, including hyperbilirubinemia, elevated alkaline phosphatase, and gamma-glutamyl transpeptidase (6). Most patients can be treated conservatively, but some cases may progress to hepatic failure (65, 66). Therefore, for the determination of treatment protocols, both treatment efficacy and potential

liver toxicity should be considered. Radiologic findings of REILD include liver parenchymal edema and hepatomegaly, which are quite nonspecific (5). In clinical practice, if a post-treatment patient shows clinical and laboratory abnormalities suggestive of liver dysfunction and does not have any evidence of disease progression or biliary obstruction on imaging studies, REILD should be highly suspected.

Radiation Pneumonitis

If excessive radioactive microspheres flow into the pulmonary artery through tumor-induced arteriovenous shunting in the liver, the lung parenchyma would be irradiated and radiation pneumonitis may develop (67). The incidence of radiation pneumonitis is less than 1% in cases where standard dosimetry is used (6). To avoid the risk of radiation pneumonitis, a pretreatment $^{99\text{m}}\text{Tc}$ -MAA scan is routinely performed to measure the lung shunt fraction, which is used in patient selection (16). If radiation pneumonitis develops, patients will present with non-productive cough, dyspnea, and fever (67). Typical CT imaging features include ill-defined, patchy opacities, and ground glass opacities in a symmetric pattern with relative sparing of the peripheral and hilar portions, resulting in “bat-wing” appearance (67). These imaging findings of the acute stage may resolve after corticosteroid treatment. If radiation pneumonitis progresses to radiation fibrosis, linear scarring, volume loss, traction bronchiectasis, and honeycombing appearance can be observed in the chronic stage (51).

Radiation Cholecystitis

Radiation cholecystitis can develop due to non-target administration of radioactive microspheres into the cystic artery and it may require cholecystectomy or percutaneous cholecystostomy (68). The reported incidence of radiation cholecystitis requiring surgery is 0–2.4% (60). This complication should be suspected in patients presenting with right upper quadrant pain, fever, and nausea occurring shortly after radioembolization, and gallbladder wall thickening and/or pericholecystic fluid collection seen on imaging studies (69). However, as mentioned earlier, gallbladder abnormalities are frequently detected on post-radioembolization follow-up imaging in patients without any symptoms (60). Indeed, clinically significant radiation cholecystitis is rare and conservative treatment is the initial management, although some refractory cases require surgery (70).

For preventing radiation cholecystitis, microspheres should be administered into the hepatic artery distal to the cystic artery whenever feasible (68). Prophylactic embolization of the cystic artery can be performed, although there are controversies about the benefit considering the low incidence of clinically significant radiation cholecystitis and increased risk of ischemic cholecystitis due to cystic artery occlusion (71). In addition, temporary occlusion of the cystic artery using a detachable coil can be attempted as it reduces microsphere uptake in the gallbladder during the radioembolization procedure and minimizes the risk of ischemic cholecystitis by removal of the coil after the procedure (72).

Gastrointestinal Ulceration

Non-target administration of radioactive microspheres into the microvasculature of the gastrointestinal tract may cause gastrointestinal ulceration (73). The incidence of gastric ulcer has been reported to range from 0.1% to 3.1% (74). This is the main rationale for prophylactic embolization of aberrant vasculatures during pretreatment hepatic angiography. Deposition of radioactive microspheres in the gastric or duodenal wall leads to direct radiation toxicity as well as chronic ischemic changes due to microvascular injury (75, 76). Gastrointestinal ulcer caused by ⁹⁰Y can present several months after treatment and can be accompanied by severe abdominal pain (77). As it seldom heals with medical treatment, surgical resection of the affected gut should be considered (73). A high index of suspicion is needed to make the diagnosis of radioembolization-associated gastrointestinal ulceration as the clinical, endoscopic, and

imaging features are nonspecific.

CONCLUSION

Radioembolization using ⁹⁰Y is being actively investigated as an effective and safe treatment option for various kinds of hepatic malignancies. As it works by delivering intense radiation to liver tumors with little embolic effect, it results in unique post-treatment imaging findings different from those following chemotherapy or chemoembolization. For tumor response assessment after radioembolization, imaging changes in size, enhancing tumor burden, and diffusion restriction as well as serum tumor markers can be useful, and a combination may improve the diagnostic accuracy. Common post-treatment benign changes such as peritumoral ring enhancement and perivascular edema should not be interpreted as tumor progression. Radioembolization can cause several complications due to the radiation effect in the surrounding structures or aberrant deposition of microspheres in the non-target organs such as gallbladder, gastrointestinal tract, and lungs. Management decisions about imaging-detected complications should be made based on the correlation of clinical symptoms and laboratory findings.

REFERENCES

1. Sangro B, Iñarrairaegui M, Bilbao JI. Radioembolization for hepatocellular carcinoma. *J Hepatol* 2012;56:464-473
2. Lee EW, Alanis L, Cho SK, Saab S. Yttrium-90 selective internal radiation therapy with glass microspheres for hepatocellular carcinoma: current and updated literature review. *Korean J Radiol* 2016;17:472-488
3. Lanza E, Donadon M, Poretti D, Pedicini V, Tramarin M, Roncalli M, et al. Transarterial therapies for hepatocellular carcinoma. *Liver Cancer* 2016;6:27-33
4. Fidelman N, Kerlan RK Jr. Transarterial chemoembolization and (90)Y radioembolization for hepatocellular carcinoma: review of current applications beyond intermediate-stage disease. *AJR Am J Roentgenol* 2015;205:742-752
5. Atassi B, Bangash AK, Bahrani A, Pizzi G, Lewandowski RJ, Ryu RK, et al. Multimodality imaging following 90Y radioembolization: a comprehensive review and pictorial essay. *Radiographics* 2008;28:81-99
6. Riaz A, Lewandowski RJ, Kulik LM, Mulcahy MF, Sato KT, Ryu RK, et al. Complications following radioembolization with yttrium-90 microspheres: a comprehensive literature review. *J Vasc Interv Radiol* 2009;20:1121-1130; quiz 1131
7. Coldwell D, Sangro B, Wasan H, Salem R, Kennedy A. General selection criteria of patients for radioembolization of liver

- tumors: an international working group report. *Am J Clin Oncol* 2011;34:337-341
8. Rosenbaum CE, Verkooijen HM, Lam MG, Smits ML, Koopman M, van Seeters T, et al. Radioembolization for treatment of salvage patients with colorectal cancer liver metastases: a systematic review. *J Nucl Med* 2013;54:1890-1895
 9. Kim HC. Radioembolization for the treatment of hepatocellular carcinoma. *Clin Mol Hepatol* 2017;23:109-114
 10. Kim DY, Han KH. Transarterial chemoembolization versus transarterial radioembolization in hepatocellular carcinoma: optimization of selecting treatment modality. *Hepatol Int* 2016;10:883-892
 11. Kim HC. Role of C-arm cone-beam CT in chemoembolization for hepatocellular carcinoma. *Korean J Radiol* 2015;16:114-124
 12. Borggreve AS, Landman AJEMC, Vissers CMJ, De Jong CD, Lam MGEH, Monninkhof EM, et al. Radioembolization: is prophylactic embolization of hepaticoenteric arteries necessary? A systematic review. *Cardiovasc Intervent Radiol* 2016;39:696-704
 13. Camacho JC, Moncayo V, Kokabi N, Reavey HE, Galt JR, Yamada K, et al. (90)Y radioembolization: multimodality imaging pattern approach with angiographic correlation for optimized target therapy delivery. *Radiographics* 2015;35:1602-1618
 14. Kao YH, Hock Tan AE, Burgmans MC, Irani FG, Khoo LS, Gong Lo RH, et al. Image-guided personalized predictive dosimetry by artery-specific SPECT/CT partition modeling for safe and effective 90Y radioembolization. *J Nucl Med* 2012;53:559-566
 15. Roshan HR, Azarm A, Mahmoudian B, Islamian JP. Advances in SPECT for optimizing the liver tumors radioembolization using yttrium-90 microspheres. *World J Nucl Med* 2015;14:75-80
 16. Braat AJ, Smits ML, Braat MN, van den Hoven AF, Prince JF, de Jong HW, et al. ⁹⁰Y hepatic radioembolization: an update on current practice and recent developments. *J Nucl Med* 2015;56:1079-1087
 17. Uliel L, Royal HD, Darcy MD, Zuckerman DA, Sharma A, Saad NE. From the angio suite to the γ -camera: vascular mapping and ^{99m}Tc-MAA hepatic perfusion imaging before liver radioembolization--a comprehensive pictorial review. *J Nucl Med* 2012;53:1736-1747
 18. Kallini JR, Gabr A, Salem R, Lewandowski RJ. Transarterial radioembolization with yttrium-90 for the treatment of hepatocellular carcinoma. *Adv Ther* 2016;33:699-714
 19. Riaz A, Gates VL, Atassi B, Lewandowski RJ, Mulcahy MF, Ryu RK, et al. Radiation segmentectomy: a novel approach to increase safety and efficacy of radioembolization. *Int J Radiat Oncol Biol Phys* 2011;79:163-171
 20. Padia SA, Kwan SW, Roudsari B, Monsky WL, Coveler A, Harris WP. Superselective yttrium-90 radioembolization for hepatocellular carcinoma yields high response rates with minimal toxicity. *J Vasc Interv Radiol* 2014;25:1067-1073
 21. Vouche M, Habib A, Ward TJ, Kim E, Kulik L, Ganger D, et al. Unresectable solitary hepatocellular carcinoma not amenable to radiofrequency ablation: multicenter radiology-pathology correlation and survival of radiation segmentectomy. *Hepatology* 2014;60:192-201
 22. Lewandowski RJ, Donahue L, Chochechanachaisakul A, Kulik L, Mouli S, Caicedo J, et al. (90) Y radiation lobectomy: outcomes following surgical resection in patients with hepatic tumors and small future liver remnant volumes. *J Surg Oncol* 2016;114:99-105
 23. Vouche M, Lewandowski RJ, Atassi R, Memon K, Gates VL, Ryu RK, et al. Radiation lobectomy: time-dependent analysis of future liver remnant volume in unresectable liver cancer as a bridge to resection. *J Hepatol* 2013;59:1029-1036
 24. Lhommel R, Goffette P, Van den Eynde M, Jamar F, Pauwels S, Bilbao JI, et al. Yttrium-90 TOF PET scan demonstrates high-resolution biodistribution after liver SIRT. *Eur J Nucl Med Mol Imaging* 2009;36:1696
 25. Pasciak AS, Bourgeois AC, McKinney JM, Chang TT, Osborne DR, Acuff SN, et al. Radioembolization and the dynamic role of (90)Y PET/CT. *Front Oncol* 2014;4:38
 26. Bagni O, D'Arienzo M, Chiaramida P, Chiacchiararelli L, Cannas P, D'Agostini A, et al. 90Y-PET for the assessment of microsphere biodistribution after selective internal radiotherapy. *Nucl Med Commun* 2012;33:198-204
 27. Fowler KJ, Maughan NM, Laforest R, Saad NE, Sharma A, Olsen J, et al. PET/MRI of hepatic 90Y microsphere deposition determines individual tumor response. *Cardiovasc Intervent Radiol* 2016;39:855-864
 28. Cosimelli M, Golfieri R, Cagol PP, Carpanese L, Sciuto R, Maini CL, et al. Multi-centre phase II clinical trial of yttrium-90 resin microspheres alone in unresectable, chemotherapy refractory colorectal liver metastases. *Br J Cancer* 2010;103:324-331
 29. Hoffmann RT, Paprottka PM, Schön A, Bamberg F, Haug A, Dürr EM, et al. Transarterial hepatic yttrium-90 radioembolization in patients with unresectable intrahepatic cholangiocarcinoma: factors associated with prolonged survival. *Cardiovasc Intervent Radiol* 2012;35:105-116
 30. Salem R, Lewandowski RJ, Mulcahy MF, Riaz A, Ryu RK, Ibrahim S, et al. Radioembolization for hepatocellular carcinoma using Yttrium-90 microspheres: a comprehensive report of long-term outcomes. *Gastroenterology* 2010;138:52-64
 31. Keppke AL, Salem R, Reddy D, Huang J, Jin J, Larson AC, et al. Imaging of hepatocellular carcinoma after treatment with yttrium-90 microspheres. *AJR Am J Roentgenol* 2007;188:768-775
 32. Miller FH, Keppke AL, Reddy D, Huang J, Jin J, Mulcahy MF, et al. Response of liver metastases after treatment with yttrium-90 microspheres: role of size, necrosis, and PET. *AJR Am J Roentgenol* 2007;188:776-783
 33. Riaz A, Kulik L, Lewandowski RJ, Ryu RK, Giakoumis Spear G, Mulcahy MF, et al. Radiologic-pathologic correlation of hepatocellular carcinoma treated with internal radiation using yttrium-90 microspheres. *Hepatology* 2009;49:1185-1193
 34. Camacho JC, Kokabi N, Xing M, Prajapati HJ, El-Rayes B, Kim

- HS. Modified response evaluation criteria in solid tumors and European Association for The Study of the Liver criteria using delayed-phase imaging at an early time point predict survival in patients with unresectable intrahepatic cholangiocarcinoma following yttrium-90 radioembolization. *J Vasc Interv Radiol* 2014;25:256-265
35. Chapiro J, Duran R, Lin M, Scherthaner R, Lesage D, Wang Z, et al. Early survival prediction after intra-arterial therapies: a 3D quantitative MRI assessment of tumour response after TACE or radioembolization of colorectal cancer metastases to the liver. *Eur Radiol* 2015;25:1993-2003
 36. Guo Y, Yaghmai V, Salem R, Lewandowski RJ, Nikolaidis P, Larson AC, et al. Imaging tumor response following liver-directed intra-arterial therapy. *Abdom Imaging* 2013;38:1286-1299
 37. Singh P, Anil G. Yttrium-90 radioembolization of liver tumors: what do the images tell us? *Cancer Imaging* 2014;13:645-657
 38. Shady W, Sotirchos VS, Do RK, Pandit-Taskar N, Carrasquillo JA, Gonen M, et al. Surrogate imaging biomarkers of response of colorectal liver metastases after salvage radioembolization using ⁹⁰Y-loaded resin microspheres. *AJR Am J Roentgenol* 2016;207:661-670
 39. Bester L, Hobbins PG, Wang SC, Salem R. Imaging characteristics following ⁹⁰yttrium microsphere treatment for unresectable liver cancer. *J Med Imaging Radiat Oncol* 2011;55:111-118
 40. Jiang T, Zhu AX, Sahani DV. Established and novel imaging biomarkers for assessing response to therapy in hepatocellular carcinoma. *J Hepatol* 2013;58:169-177
 41. Taouli B, Koh DM. Diffusion-weighted MR imaging of the liver. *Radiology* 2010;254:47-66
 42. Kokabi N, Camacho JC, Xing M, Qiu D, Kitajima H, Mittal PK, et al. Apparent diffusion coefficient quantification as an early imaging biomarker of response and predictor of survival following yttrium-90 radioembolization for unresectable infiltrative hepatocellular carcinoma with portal vein thrombosis. *Abdom Imaging* 2014;39:969-978
 43. Schmeel FC, Simon B, Sabet A, Luetkens JA, Träber F, Schmeel LC, et al. Diffusion-weighted magnetic resonance imaging predicts survival in patients with liver-predominant metastatic colorectal cancer shortly after selective internal radiation therapy. *Eur Radiol* 2017;27:966-975
 44. Joo I, Lee JM, Han JK, Choi BI. Intravoxel incoherent motion diffusion-weighted MR imaging for monitoring the therapeutic efficacy of the vascular disrupting agent CKD-516 in rabbit VX2 liver tumors. *Radiology* 2014;272:417-426
 45. Koh DM, Collins DJ, Orton MR. Intravoxel incoherent motion in body diffusion-weighted MRI: reality and challenges. *AJR Am J Roentgenol* 2011;196:1351-1361
 46. Yang SH, Lin J, Lu F, Han ZH, Fu CX, Lv P, et al. Evaluation of antiangiogenic and antiproliferative effects of sorafenib by sequential histology and intravoxel incoherent motion diffusion-weighted imaging in an orthotopic hepatocellular carcinoma xenograft model. *J Magn Reson Imaging* 2017;45:270-280
 47. Pieper CC, Meyer C, Sprinkart AM, Block W, Ahmadzadehfar H, Schild HH, et al. The value of intravoxel incoherent motion model-based diffusion-weighted imaging for outcome prediction in resin-based radioembolization of breast cancer liver metastases. *Onco Targets Ther* 2016;9:4089-4098
 48. Pieper CC, Sprinkart AM, Meyer C, König R, Schild HH, Kukuk GM, et al. Evaluation of a simplified intravoxel incoherent motion (IVIM) analysis of diffusion-weighted imaging for prediction of tumor size changes and imaging response in breast cancer liver metastases undergoing radioembolization: a retrospective single center analysis. *Medicine (Baltimore)* 2016;95:e3275
 49. Memon K, Kulik L, Lewandowski RJ, Wang E, Ryu RK, Riaz A, et al. Alpha-fetoprotein response correlates with EASL response and survival in solitary hepatocellular carcinoma treated with transarterial therapies: a subgroup analysis. *J Hepatol* 2012;56:1112-1120
 50. Hipps D, Ausania F, Manas DM, Rose JD, French JJ. Selective interarterial radiation therapy (SIRT) in colorectal liver metastases: how Do we monitor response? *HPB Surg* 2013;2013:570808
 51. Kallini JR, Miller FH, Gabr A, Salem R, Lewandowski RJ. Hepatic imaging following intra-arterial embolotherapy. *Abdom Radiol (NY)* 2016;41:600-616
 52. Ibrahim SM, Nikolaidis P, Miller FH, Lewandowski RJ, Ryu RK, Sato KT, et al. Radiologic findings following ⁹⁰Y radioembolization for primary liver malignancies. *Abdom Imaging* 2009;34:566-581
 53. Bhangoo MS, Karnani DR, Hein PN, Giap H, Knowles H, Issa C, et al. Radioembolization with Yttrium-90 microspheres for patients with unresectable hepatocellular carcinoma. *J Gastrointest Oncol* 2015;6:469-478
 54. Park MJ, Kim SY, Yoon SM, Kim JH, Park SH, Lee SS, et al. Stereotactic body radiotherapy-induced arterial hypervascularity of non-tumorous hepatic parenchyma in patients with hepatocellular carcinoma: potential pitfalls in tumor response evaluation on multiphase computed tomography. *PLoS One* 2014;9:e90327
 55. Lock M, Malayeri AA, Mian OY, Mayr NA, Herman JM, Lo SS. Computed tomography imaging assessment of postexternal beam radiation changes of the liver. *Future Oncol* 2016;12:2729-2739
 56. Herfarth KK, Hof H, Bahner ML, Lohr F, Höss A, van Kaick G, et al. Assessment of focal liver reaction by multiphase CT after stereotactic single-dose radiotherapy of liver tumors. *Int J Radiat Oncol Biol Phys* 2003;57:444-451
 57. Marin D, Cappabianca S, Serra N, Sica A, Lassandro F, D'Angelo R, et al. CT appearance of hepatocellular carcinoma after locoregional treatments: a comprehensive review. *Gastroenterol Res Pract* 2015;2015:670965
 58. Kulik LM, Atassi B, van Holsbeeck L, Souman T, Lewandowski RJ, Mulcahy MF, et al. Yttrium-90 microspheres (TheraSphere) treatment of unresectable hepatocellular carcinoma: downstaging to resection, RFA and bridge to transplantation. *J Surg Oncol* 2006;94:572-586

59. Braat AJ, Huijbregts JE, Molenaar IQ, Borel Rinkes IH, van den Bosch MA, Lam MG. Hepatic radioembolization as a bridge to liver surgery. *Front Oncol* 2014;4:199
60. Prince JF, van den Hoven AF, van den Bosch MA, Elschot M, de Jong HW, Lam MG. Radiation-induced cholecystitis after hepatic radioembolization: do we need to take precautionary measures? *J Vasc Interv Radiol* 2014;25:1717-1723
61. Yu MH, Kim YJ, Park HS, Jung SI, Jeon HJ. Imaging patterns of intratumoral calcification in the abdominopelvic cavity. *Korean J Radiol* 2017;18:323-335
62. Sharma RA, Van Hazel GA, Morgan B, Berry DP, Blanshard K, Price D, et al. Radioembolization of liver metastases from colorectal cancer using yttrium-90 microspheres with concomitant systemic oxaliplatin, fluorouracil, and leucovorin chemotherapy. *J Clin Oncol* 2007;25:1099-1106
63. Riaz A, Awais R, Salem R. Side effects of yttrium-90 radioembolization. *Front Oncol* 2014;4:198
64. Gil-Alzugaray B, Chopitea A, Iñarrairaegui M, Bilbao JI, Rodriguez-Fraile M, Rodriguez J, et al. Prognostic factors and prevention of radioembolization-induced liver disease. *Hepatology* 2013;57:1078-1087
65. Hamoui N, Ryu RK. Hepatic radioembolization complicated by fulminant hepatic failure. *Semin Intervent Radiol* 2011;28:246-251
66. Kuo JC, Tazbirkova A, Allen R, Kosmider S, Gibbs P, Yip D. Serious hepatic complications of selective internal radiation therapy with yttrium-90 microsphere radioembolization for unresectable liver tumors. *Asia Pac J Clin Oncol* 2014;10:266-272
67. Wright CL, Werner JD, Tran JM, Gates VL, Rikabi AA, Shah MH, et al. Radiation pneumonitis following yttrium-90 radioembolization: case report and literature review. *J Vasc Interv Radiol* 2012;23:669-674
68. Padia SA, Lewandowski RJ, Johnson GE, Sze DY, Ward TJ, Gaba RC, et al. Radioembolization of hepatic malignancies: background, quality improvement guidelines, and future directions. *J Vasc Interv Radiol* 2017;28:1-15
69. Parakh S, Gananadha S, Allen R, Yip D. Cholecystitis after yttrium-90 resin microsphere radioembolization treatment: clinical and pathologic findings. *Asian J Surg* 2016;39:144-148
70. Sag AA, Savin MA, Lal NR, Mehta RR. Yttrium-90 radioembolization of malignant tumors of the liver: gallbladder effects. *AJR Am J Roentgenol* 2014;202:1130-1135
71. Hickey R, Lewandowski RJ. Hepatic radioembolization complicated by radiation cholecystitis. *Semin Intervent Radiol* 2011;28:230-233
72. Choi JW, Yoo MY, Kim HC, Paeng JC, Kim YJ, Chung JW. Prophylactic temporary occlusion of the cystic artery using a fibered detachable coil during 90y radioembolization. *Cardiovasc Intervent Radiol* 2017;40:1624-1630
73. South CD, Meyer MM, Meis G, Kim EY, Thomas FB, Rikabi AA, et al. Yttrium-90 microsphere induced gastrointestinal tract ulceration. *World J Surg Oncol* 2008;6:93
74. Kallini JR, Gabr A, Thorlund K, Baliyepalli C, Ayres D, Kanters S. Comparison of the adverse event profile of TheraSphere[®] with SIR-Spheres[®] for the treatment of unresectable hepatocellular carcinoma: a systematic review. *Cardiovasc Intervent Radiol* 2017;40:1033-1043
75. Sun B, Lapetino SR, Diffalha SA, Yong S, Gaba RC, Bui JT, et al. Microvascular injury in persistent gastric ulcers after yttrium-90 microsphere radioembolization for liver malignancies. *Hum Pathol* 2016;50:11-14
76. Veloso N, Brandão C, Gonçalves B, Costa L, Coimbra N, Jacome M, et al. Gastroduodenal ulceration following liver radioembolization with yttrium-90. *Endoscopy* 2013;45 Suppl 2 UCTN:E108-E109
77. Naymagon S, Warner RR, Patel K, Harpaz N, Machac J, Weintraub JL, et al. Gastroduodenal ulceration associated with radioembolization for the treatment of hepatic tumors: an institutional experience and review of the literature. *Dig Dis Sci* 2010;55:2450-2458